

Efficient transmission control based on carrier accumulation in silicon slot photonic-crystal waveguide as an embedded layer for board level optical interconnects

Xiaonan Chen¹, Lanlan Gu², and Ray T. Chen^{1*}

Microelectronic Research Center, Department of Electrical and Computer Engineering,

¹The University of Texas at Austin, Austin, TX 78758, USA

²Omega Optics Inc, Austin, TX 78758, USA

*** Email: chen@ece.utexas.edu**

ABSTRACT

We experimentally demonstrate an all-silicon optical transmission controller based on a semiconductor-oxide-semiconductor capacitor embedded in a slot photonic-crystal waveguide. We incorporate a multimode interference-based structure to reduce the coupling loss induced by the waveguide mode mismatch. We perform a detailed DC characterization of the electro-optic device including the DC modulation test and the evaluation of the resistance-capacitance constant. The measured modulation curve is in good agreement with our theoretical analysis. Calculation of the effective index change indicates as much as 30 times efficiency enhancement compared with the slotted silicon rib waveguide. Such a waveguide layer can serve as the active layer for fully embedded optical interconnect architecture with minimum power consumption.

Keywords: all-silicon, transmission control, slot photonic crystal waveguide.

I. INTRODUCTION

Silicon has been considered as an attractive material option for low-cost photonic circuits. In contrast to those conventional optoelectronic components fabricated from III-V semiconductor compounds or electro-optic materials such as lithium niobate and nonlinear organic polymers, all-silicon based optical devices offer opportunities for monolithic integration with advanced electronic circuits on a single silicon substrate. In the past few years, high-speed silicon optical modulator [1-3] has been one of the significant advances in pushing device performance for applications ranging from telecommunication down to chip-to-chip interconnection. Nevertheless, it is challenging to achieve efficient optical intensity modulation in silicon because the material does not exhibit any appreciable electro-optic effect [4]. Therefore, a straightforward integration with high-frequency silicon modulator usually requires centimeter-scale active region and inevitable complex electrode design. In order to meet the miniaturization demand of high performance micro- / nano- very-large-scale-integration (VLSI) photonic circuit, it would be desirable to achieve more efficient transmission control from structural innovation and optimization. Here we describe an approach based on a semiconductor-oxide-semiconductor (SOS) capacitor embedded in a silicon slot photonic crystal waveguide that can produce more efficient optical phase modulation compared with those built in conventional silicon strip waveguides: we propose a feasible solution to incorporate the novel structure with common waveguide interface and demonstrate an all-silicon optical transmission controller with 300 μ m interaction

length and 6V turn-off voltage.

II. SILICON SLOT PHOTONIC CRYSTAL WAVEGUIDES INCORPORATING AN INTERFERENCE-BASED COUPLING STRUCTURE

The light transmission controller presented here is based on a conventional Mach-Zehnder interferometer with a SOS capacitor embedded in each of the two arms, as shown in Fig. 1. In order to obtain higher controlling performance, we design and fabricate a line defect photonic crystal waveguide with slow photon effect [2]. The width of the defect region is $\sim 1.2\mu\text{m}$, the center slot width is $\sim 0.1\mu\text{m}$, the slab height is $\sim 0.24\mu\text{m}$ and the lattice constant of the hexagonal structure is $\sim 0.4\mu\text{m}$. Both modeling and experimental data confirm the waveguide operates with a single transmission mode at the wavelength around $1.55\mu\text{m}$ [5]. Simulation indicates the guided mode is a quasi-transverse-electric mode with greatly reduced group velocity near the band edge.

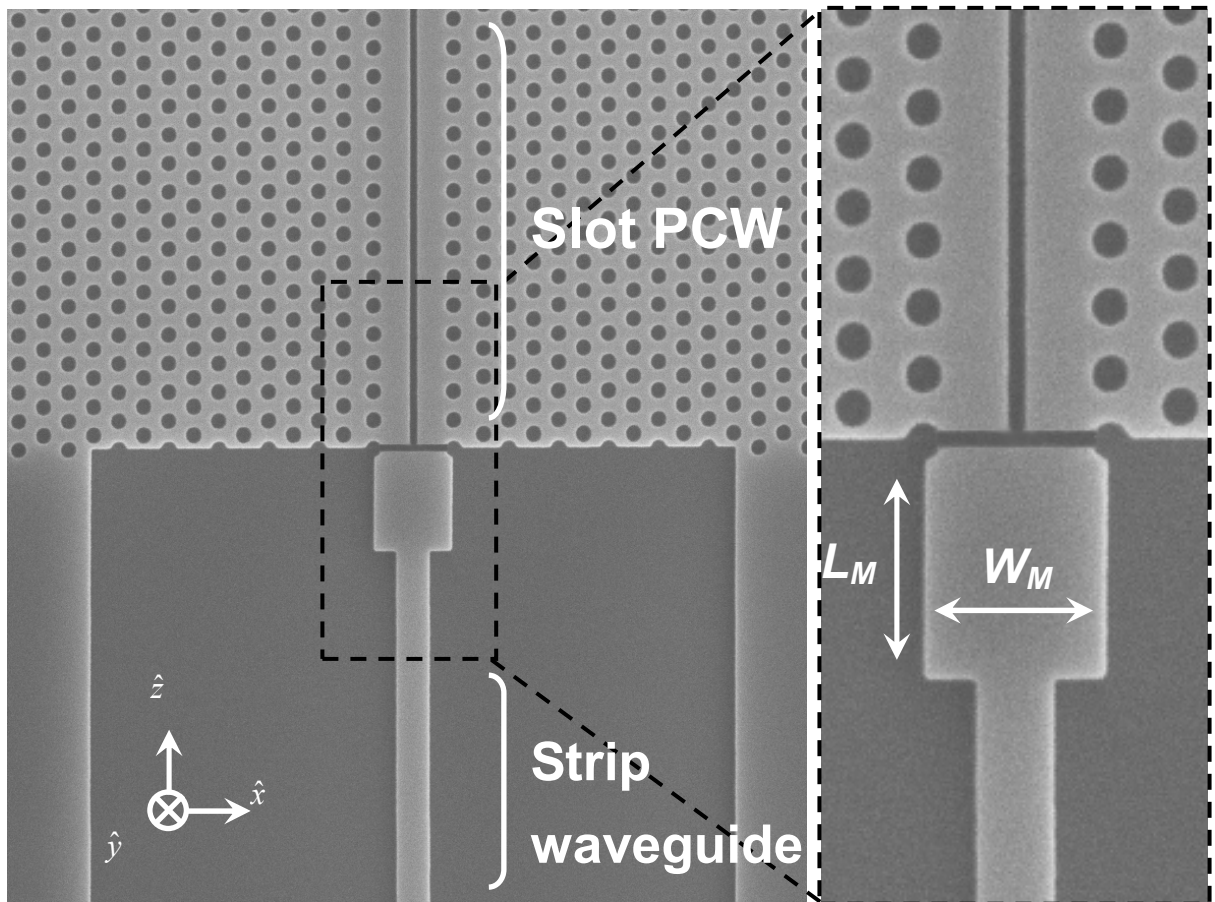


Fig. 1. Line defect structure with an oxide slot embedded in a photonic crystal slab. The slot photonic crystal waveguide and the silicon strip waveguide are combined by a multimode interference-based coupling structure. The interference length L_M and the waveguide width W_M decide the optical mode profile at the interface as well as the coupling efficiency.

We then focus on designing the multimode interference-based coupling structure to achieve practical output power level at the end of the active waveguide region. The input strip waveguide is centered with respect to the multimode

section and therefore excites the symmetric modes with tunable phase difference. Parameter optimization indicates the best coupling efficiency is reached when the phase difference in the multimode section is close to π . Further experimental comparison confirms such coupling structure enhances the coupling efficiency by 20dB over 35nm optical bandwidth centered on $1.55\mu\text{m}$ [5]. An insulation gap is introduced in the final device pattern to create strong parallel electric field for carrier accumulation.

III. ELECTRICAL CHARACTERIZATION AND PERFORMANCE EVALUATION

The final device with electrodes deposited at both sides of the waveguide region is shown by a microscopic top view in Fig. 2(a). To simplify the device fabrication flow and to limit the additional optical absorption from the sandwiched silicon layer, we implement a bulk implantation on the silicon-on-insulator (SOI) wafer with 1×10^{17} p-doping concentration. We choose aluminum as the electrode material to achieve acceptable contact resistance. Measurement shows the final resistance after 900°C thermal annealing is below $5\text{k}\Omega$.

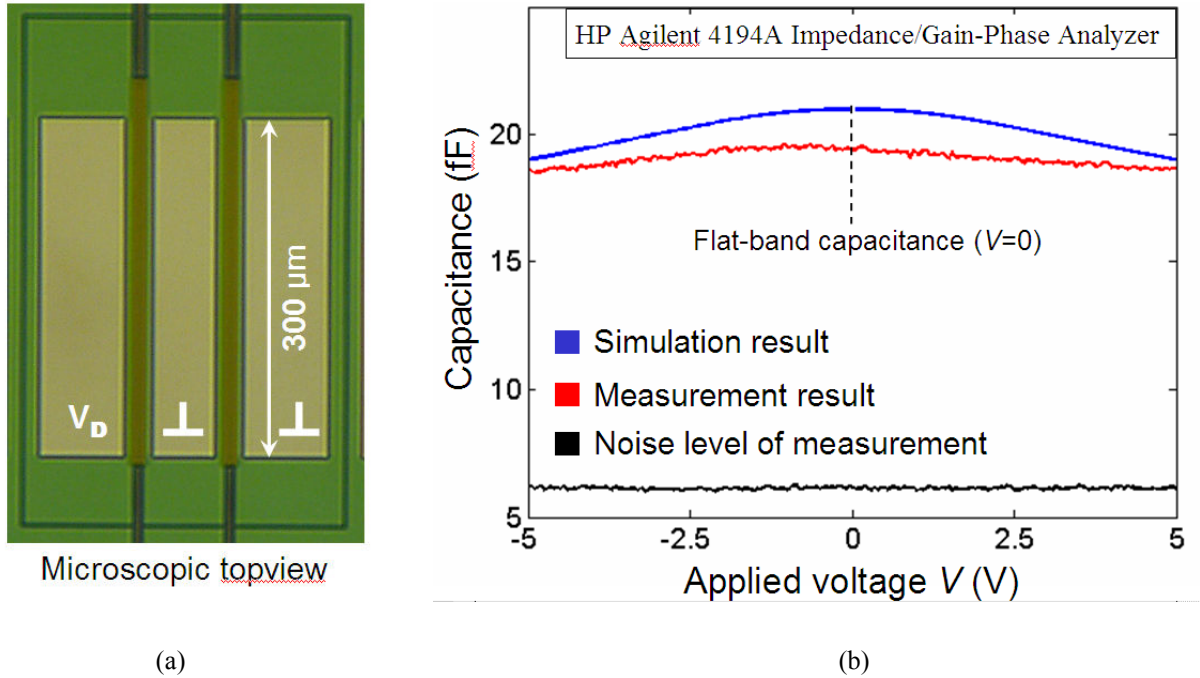


Fig. 2. (a) Microscopic top view of the symmetric Mach-Zehnder interferometer containing two SOS-capacitor-based phase shifters. (b) Simulation and measurement result of device capacitance as a function of the applied voltage.

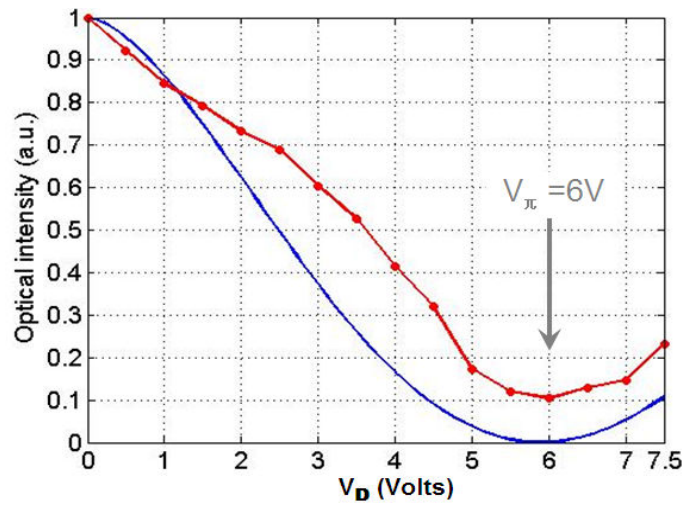
We characterize the electrical properties of the device using a HP-Agilent 4191A impedance/gain-phase analyzer. As given by Fig. 2(b), the noise level of the capacitance measurement is ~ 6 femtofarad. We simulate the capacitance-voltage curve and compare with the measurement result. The deviation of flat-band capacitance is due to positive oxide charges trapped in the center spin-on-glass trench. The curve slope difference is induced by various interface traps around the gate oxide. The negligible asymmetry stems from doping fluctuation and fabrication defects.

Based on the measured electrical parameters, calculation shows the resistance-capacitance time constant of the active

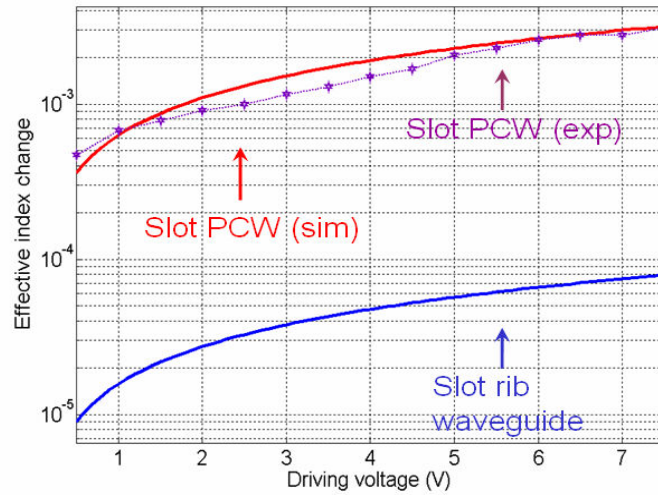
arm is below 120ps. Doping profile modification would further reduce the time constant and make the slot waveguide-based silicon structure as a good candidate to realize high-speed transmission control.

IV. OPTICAL CHARACTERIZATION AND EFFICIENCY COMPARISON

Transmission control based on Mach-Zehnder interferometer requires dynamic phase shift between the two waveguide arms. The phase change in line defect-embedded photonic crystal waveguides depends on the mode group velocity, the band shift and the total interaction length. Here we apply carrier accumulation-induced plasma dispersion effect to generate the expected band shift. Fig. 3(a) shows the measured modulation curve and the simulation result. Both of them indicate $\sim 6V$ driving voltage is required to generate the π -phase shift between two interference arms. The evaluation of band shift distance is based on the plane-wave expansion (PWE) method.



(a)



(b)

Fig. 3. (a) DC modulation curve. (b) Effective index change induced by different driving voltage.

In order to compare the efficiency of transmission control, we calculate the effective index change Δn_{eff} of both slot photonic crystal waveguide and slot rib waveguide, as shown in Fig. 3(b). With different driving voltage applied, the slot photonic crystal waveguide always provides as much as 30 times Δn_{eff} enhancement compared with the slot rib waveguide. The significant enhancement stems from the slow light effect of the photonic crystal waveguide. Power consumption and device size needed to modulate an optical signal are thus significantly reduced. This advantage is crucial for fully embedded board level interconnect [6-9] as indicated in Figure 4 where heat dissipation due to the fully embedded structure is a paramount concern.

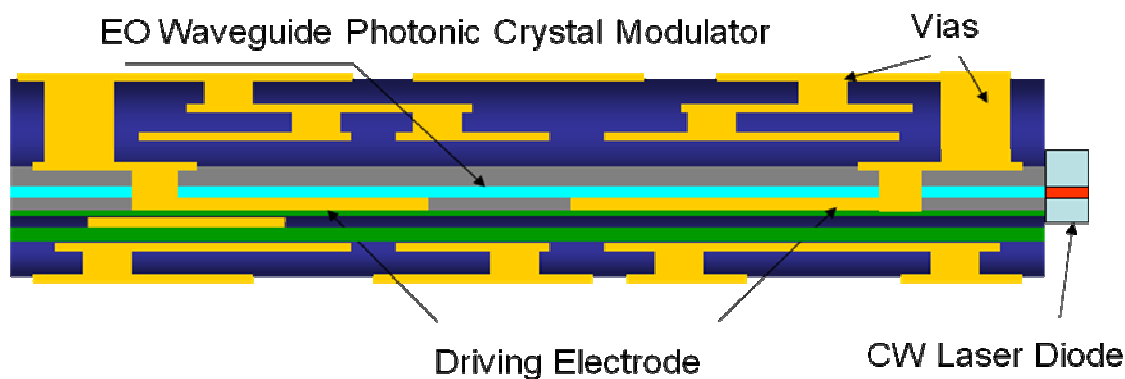


Figure 4 Employment of photonic crystal waveguide modulator in fully embedded board level optical interconnect with indirect modulation scheme where a CW laser is attached to provide constant light source [6-9]

V. CONCLUSION

A carrier accumulation-based efficient transmission controller operating at communication wavelength ($1.55\mu\text{m}$) is demonstrated. A multimode interference-based coupling structure is incorporated to implement feasible waveguide combination. The final device is characterized based on electrical and optical performance. The measured device properties indicate that such structural innovation would be a practical option to achieve efficient transmission control based on an all-silicon optical component.

ACKNOWLEDGMENTS

This research is supported in part by AFOSR and DARPA. The devices were fabricated at UT MRC with nanofabrication facilities partially supported under NSF's NNIN program. We thank the CNM of UT Austin, Welch Foundation and SPRING for partial support of the Dual Beam FIB/SEM usage.

REFERENCES

1. A. Liu, R. Jones, L. Liao, D. Samara-Rubio, D. Rubin, O. Cohen, R. Nicolaescu, and M. Paniccia., "A high-speed silicon optical modulator based on a metal-oxide-semiconductor capacitor," *Nature* 427, 615 (2004)

Invited Paper

2. Y. Jiang, W. Jiang, L. Gu, X. Chen, and R. T. Chen, "80-micron interaction length silicon nanophotonic crystal waveguide modulator," *Appl. Phys. Lett.*, 87, 221105 (2005).
3. L. Liao, D. Samara-Rubio, M. Morse, A. Liu, D. Hodge, D. Rubin, U. D. Keil and T. Franck, "High speed silicon Mach-Zehnder modulator," *Optics Express*, vol.13, 3129 (2005).
4. R. A. Soref and B. R. Bennett, "Electrooptical effects in silicon," *IEEE J. Quantum Electron.* QE-23, 123-129 (1987).
5. X. Chen, W. Jiang, J. Chen, L. Gu, and R. T. Chen, "20dB-enhanced coupling to slot photonic crystal waveguide using multimode interference coupler," accepted by *Applied Physics Letters* (2007).
6. R. T. Chen, et al, "Fully Embedded Board level Guided-wave Optoelectronic Interconnects," Invited paper, Proceedings of IEEE, Vol.88, pp.780-793 (2000).
7. Choi, C.; Lin, L.; Yujie Liu; Jinho Choi; Li Wang; Haas, D.; Magerat, J.; Chen, R. T., "Flexible optical waveguide film fabrications and optoelectronic devices integration for fully embedded board-level optical interconnects", *Lightwave Technology, Journal of*, Volume: 22, Issue: 9, Sept. 2004, Pages:2168 – 2176
8. Choi C, Lin L, Liu YJ, Ray T. Chen, " Performance analysis of 10- μ m-thick VCSEL array in fully embedded board level guided-wave optoelectronic interconnects," *J LIGHTWAVE TECHNOL* 21 (6): 1531-1535 JUN 2003
9. J. H. Choi, L.Wang, H. Bi and R. T. Chen, "Effects of Thermal-Via Structures on Thin Film VCSELs for Fully Embedded Board-Level Optical Interconnection System," *IEEE Journal of Selected Topics on Quantum Electronics*, Special Issue on Optoelectronic Packaging, pp. 1060-1065, 2006.